Advanced interferometric profile measurements through refractive media

Stephan T. Koev and Reza Ghodssi
MEMS Sensors and Actuators Laboratory (MSAL), Department of Electrical and Computer Engineering, Institute for Systems Research, University of Maryland, College Park, Maryland 20742, USA

(Received 28 June 2008; accepted 15 August 2008; published online 11 September 2008)

Optical profilers are valuable tools for the characterization of microelectromechanical systems (MEMSs). They use phase sifting interferometry (PSI) or vertical scanning interferometry to measure the topography of microscale structures with nanometer resolution. However, for many emerging MEMS applications, the sample needs to be imaged while placed in a liquid or in a package with a glass window. The increased refractive index of the transparent medium degrades the interference image contrast and prevents any measurement of the sample. We report on the modification of a Veeco NT1100 optical profiler to enable PSI measurements through refractive media. This approach can be applied to any other optical profiler with PSI capability. The modification consists in replacing the original illumination source with a custom-built narrow linewidth source, which increases the coherence length of the light and the contrast of the interference image. We present measurements taken with the modified configuration on samples covered with 3 mm water or 500 μm glass, and we compare them to measurements of uncovered samples. We show that the measurement precision is only slightly reduced by the water and glass, and that it is still sufficiently high for typical MEMS applications. The described method can be readily used for measuring through other types and thicknesses of refractive materials. © *2008 American Institute of Physics.* [DOI: 10.1063/1.2979006]

I. INTRODUCTION

Optical profilers are specialized microscopes with interferometric objectives, charge coupled device (CCD) cameras, and image processing software. They are capable of measuring the heights of samples with nanometer resolution in a noncontact manner. For this reason, optical profilers have become the leading tools for wide-area three-dimensional characterization of microelectromechanical systems (MEMSs).[1–4] Although other methods exist for the noncontact measurements of microscale device heights, the optical profiler has clear advantages. For example, confocal microscopes[5,6] at low magnifications appropriate to MEMS have vertical resolution on the order of hundreds of nanometers (compared to several nanometers for interferometric profilers). Scanning electron microscopes (SEMs) have vertical resolution close to that of the profilers, but they require the sample to be cleaved, making the measurement destructive. Also, the SEM provides height measurements only along the cleaved edge, while the optical profiler generates a continuous height map of the device surface.

A simplified schematic of a typical optical profiler operating in phase shifting interferometry (PSI) mode is shown in Fig. 1. Light passing through a microscope objective is split into two beams: a sample beam and a reference beam. The beams reflect off the sample surface and off a reference mirror, combine again, go through the objective, and form a magnified interference image of the sample on a CCD array. The local intensity of the image depends on the phase difference between the reference and the sample beams, which in turn depends on the distance from the beam splitter to the points on the sample surface. A software algorithm determines the phase difference for each pixel and calculates a map of the sample height.

The interference image is formed only if the reference beam and the sample beam are temporally coherent. For this reason, the position of the reference mirror is such that the optical path lengths of the two beams are closely matched. However, if a slice of transparent material is placed above the sample, the sample beam experiences an added phase sift due to the higher refractive index. The two beams become mismatched, and the interference image contrast diminishes or even disappears, preventing any measurement of sample height. The exact effect of the added transparent material depends on the spectral width of the light. Commercially available profilers have illumination sources with appreciable linewidth, and even 100 μm of glass would render the sample immeasurable. A more detailed discussion of this limitation is given in Sec. II.

Many MEMS applications require samples to be measured through refractive materials. Some devices, such as resonators, gyroscopes, switches, and display elements, are sealed in transparent packages to isolate them from environmental humidity and pressure.[7,8] It is necessary to characterize their static properties and dynamic behavior inside the controlled package as they would behave very differently outside of it. Other devices, such as actuators and manipulators, normally operate completely immersed in liquid[9,10] because they are used to move dissolved particles or biological cells. The liquid has a significant impact on their operation due to material swelling and viscous drag forces; this requires measurement of the actuator response inside the liq-

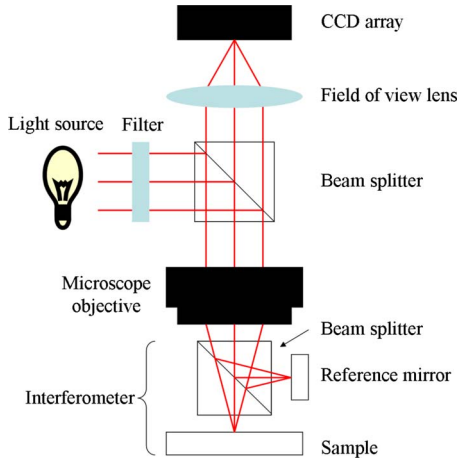

FIG. 1. (Color online) Schematic of an optical profiler based on PSI. Light reflected from a reference mirror and light reflected from the sample are combined to form an interference image. The image is digitized by a CCD and processed by software to determine the sample profile.

uid. Finally, some MEMS sensors are used to detect binding of biomolecules or the products of chemical reactions by means of the mechanical strain they cause.[11,12] These biochemical events occur in the solution phase, and the sensor displacement must be measured in liquid. Although optical profilers are an excellent metrology tool for MEMS, they have not been useful for the applications discussed here due to the presence of refractive media.

We have surveyed a number of optical profiler manufacturers, including Veeco Instruments Inc., Zygo Corp., Tamar Technology, Taylor Hobson Ltd., Solarius Development Inc., Fogale Nanotech, and ST Instruments. Among these companies, only Veeco Instruments Inc. offers the capability of measuring through some refractive media: the through transmissive media objective (TTM). Their approach is based on an interferometric objective with a movable reference mirror. This allows the reference beam path length to be adjusted to match the sample beam path length when a refractive material is placed above the sample. Due to material dispersion, however, simple motion of the mirror cannot match the path lengths for all the frequencies of light present. The objective also has a slot for inserting a piece of the refractive material from the sample into the reference path; this compensates for the dispersion and the path lengths can be well matched. Excellent measurement results through glass have been demonstrated using the TTM objective.[13–15] However, this approach still has limitations. Measurements through glass work well only if the same thickness of the same type of glass used in the MEMS device packaging is inserted in the reference path. The glass needs to be cut to an exact shape to fit into the objective, leading to a long setup time for each new sample. Measurements through liquid are more problematic; inserting liquid in the reference path and making it of the same thickness as the liquid in the sample path would be quite challenging. Even if this is achieved, liquid thickness tends to decrease due to evaporation, and the objective would need to be continually adjusted. Finally, the TTM objectives have a reduced working distance compared to conventional interferometric objectives due to the added compensation parts.

Our approach to the problem of measuring through refractive media is to use coherent light from a laser diode as the illumination source of the profiler. This allows the reference and sample beams to remain temporally coherent even if they have mismatched path lengths. The contrast of the interference image is enhanced, and a PSI measurement can be performed with a transparent material covering the sample. The laser illumination has high spatial coherence and introduces speckle noise.[16] For this reason, we use a custom-built rotating diffuser to decohere the laser light spatially and reduce the speckle while preserving the temporal coherence.

Laser illumination is common in the field of the Fizeau interferometry.[17,18] The Fizeau configuration has a large optical path difference between the sample beam and the reference beam and normally requires coherent light. Fizeau interferometers are typically used for measuring macroscale optical components (lenses, mirrors, plates) rather than MEMS features. Some microscopic Fizeau profilers with laser illumination and rotating diffusers were developed previously.[19,20] These instruments should, in principle, be able to measure MEMS features through transparent materials, but that was not demonstrated directly. Also, there are currently no commercially available instruments of this type.

Our method for measuring through transparent materials is compatible with commercially available microscopic profilers, which are normally based on the Michelson, Mireau, or Linnik interferometer configuration. The method does not require adjustable objectives like the TTM discussed above; conventional profiler objectives with fixed reference mirrors and without dispersive compensation are used. The main limitation of our approach is that it is only applicable to PSI. Optical profilers also have a vertical scanning interferometry (VSI) mode, which has a larger vertical range.[21] The operating principle of VSI requires white light, and it cannot work with a coherent light source. However, PSI is quite useful for a variety of MEMS applications.

In this paper, we describe the implementation of the custom-built laser illumination source and its use with a Veeco NT1100 profiler (Veeco Instruments Inc., Tucson, AZ) to measure samples covered by water or glass. The results are compared to measurements of the uncovered sample obtained with the original instrument light source.

II. EFFECT OF LIGHT SPECTRUM ON INTERFERENCE IMAGE

In this section, we take a more detailed look at the principle of PSI and the influence of the light spectrum on the measurements. Assuming a perfectly monochromatic light source with frequency v, the intensity of the interference image $I(x,y)$ is given by Eq. (1). Here, $I_1(x,y)$ and $I_2(x,y)$ are the intensities of the sample image and the reference mirror image, respectively; $\tau(x,y)$ is the time shift between the sample and reference beams given by Eq. (2). The numerator in Eq. (2) is referred to as the optical path difference (OPD); $d_1(x,y)$ and $d_2(x,y)$ are the distances from the beam

TABLE I. Calculated coherence length of different light sources and corresponding thicknesses of transparent material covering the sample. The first three sources are standard on the Veeco NT1100 profiler. The fourth source is an external laser diode with conservatively estimated linewidth (typical linewidth is much smaller).

Light source	Linewidth	Coherence length	Max. water thickness	Max. glass thickness
Unfiltered	300 nm	1.4 μm	2.1 μm	1.5 μm
Filtered high magnification	40 nm	10.6 μm	16.0 μm	11.2 μm
Filtered low magnification	3 nm	140 μm	210 μm	150 μm
Laser diode (typical)	1 pm	420 mm	640 mm	450 mm

splitter to the sample surface and the reference mirror, respectively; n_1 and n_2 are the refractive indices of each medium,

$$I = I_1 + I_2 + 2\sqrt{I_1 I_2}\cos(2\pi\nu\tau), \tag{1}$$

$$\tau = \frac{2(d_1 n_1 - d_2 n_2)}{c} = \frac{\text{optical path difference}}{c}. \tag{2}$$

The intensity I is acquired from the CCD image and τ is calculated from it (in practice, several images are taken with slightly different d_1 to eliminate the unknowns I_1 and I_2). Since d_2 is known, τ yields d_1, which is effectively a height map of the sample surface.

The discussion above is oversimplified because practical light sources are not monochromatic. The intensity of the interference pattern resulting from a light source with arbitrary spectral width is given by Eq. (3), where $g(\tau)$ is the autocorrelation function. For spectrally narrow sources with linewidth much smaller than the central frequency ($\Delta\nu \ll \nu_0$), Eq. (3) simplifies to Eq. (4),

$$I = I_1 + I_2 + 2\sqrt{I_1 I_2}\,\mathrm{Re}\{g(\tau)\}, \tag{3}$$

$$I \approx I_1 + I_2 + 2\sqrt{I_1 I_2}|g(\tau)|\cos(2\pi\nu_0\tau). \tag{4}$$

In the case of monochromatic light, the autocorrelation function is $g(\tau)=\exp(i2\pi\nu\tau)$ and the intensity reduces to Eq. (1). However, in the general case, $g(\tau)$ is a decreasing function with maximal value at $\tau=0$ and negligible value for $\tau > \tau_c$. Here, τ_c is the coherence time, which is related to the linewidth of the light source by $t_c \approx 1/\Delta\upsilon$; the corresponding coherence length is $l_c = c\tau_c$. If the OPD between the sample and reference beams increases beyond the coherence length, the third term in Eq. (4) vanishes, and the sample height can no longer be determined from the image intensity.

For normal operation of the optical profiler, OPD$\approx$0 when the sample is in focus (assuming the sample height variations are not too large). However, if the sample is covered with transparent material, the OPD significantly increases due to the refractive index differences between the sample and reference paths [Eq. (2)]. The impact of this increase on the measurement capability depends on the coherence length of the source. Clearly, it is possible to improve the allowable thickness of the transparent material by increasing the coherence length, i.e., reducing the linewidth.

Table I lists coherence lengths for several different sources along with the calculated maximum allowable thickness of glass or water covering the sample. The first three sources are available on the Veeco NT1100 profiler used in this work. The white light source is an unfiltered incandescent light bulb; the 40 and 3 nm sources are obtained by filtering the white light. The maximum thicknesses of transparent materials are very small and unusable for practical applications, even for the 3 nm linewidth source. Water layers less than 200 μm thick evaporate spontaneously, and glass layers less than 150 μm thick are too fragile. The 3 nm filter actually attenuates the light too much and is therefore available only for low magnifications. The fourth entry in Table I is an example of a hypothetical laser source. The given linewidth of 1 pm is achievable even by low-cost semiconductor lasers.[22] This should result in sufficiently coherent illumination for any practical thickness of sample packaging or liquid.

It should be noted that there are other complications caused by the refractive material covering the sample in addition to the increase in OPD. The image is distorted because the Abbe sine condition for the objective is violated.[23] Also, the sample and reference images are mismatched in size due to the different path lengths of the divergent sample and reference beams, leading to reference phase error. The impact of these effects on the PSI measurement is difficult to predict and requires knowledge of the transfer function of the objective. Qualitatively, it is expected that the use of higher numerical aperture (NA) objectives and thicker packaging materials will lead to more distortion and phase error. However, our initial experiments showed that these effects are small for moderate thicknesses of packaging materials, and that the loss of coherence due to the increase in OPD is indeed the main problem. For example, even the high NA objectives of the Veeco NT1100 could resolve samples covered by 3 mm of water, which is sufficient for immersing a MEMS device completely.

III. IMPLEMENTATION OF NARROW LINEWIDTH LIGHT SOURCE

Lasers have the unique capability of outputting high intensities over very narrow linewidths. However, laser beams are both spatially and temporally coherent. The spatial coherence is highly undesirable for this application because it results in a speckled image. As a coherent wavefront scatters off the sample surface, secondary wavefronts are generated that have a constant phase relationship with each other. They interfere and create a random-looking interference pattern known as speckle. This pattern severely degrades the sample image and prevents any interferometric measurements of heights.

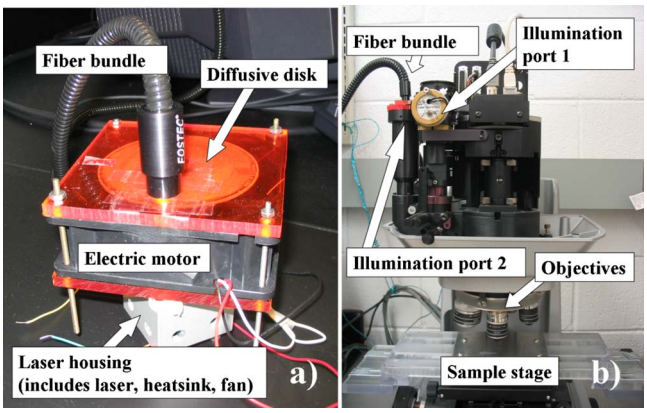

FIG. 2. (Color online) (a) Custom-made laser illumination source with a rotating diffusive disk. Output light is coupled to a fiber bundle. (b) Fiber bundle entering the secondary illumination port of the Veeco NT1100 profiler. The instrument has two illumination ports, facilitating transition between the original and custom-made sources.

Several methods have been demonstrated to reduce the speckle. Some authors have used optical feedback to trigger laser mode hopping and average out the interference pattern.[16] Unfortunately, this approach greatly reduces the temporal coherence of the light and would be counterproductive for our application. Others have demonstrated the use of mechanical motion to randomize the laser beam wavefront over space and time.[19,24,25] For example, the light is passed through a multimode optical fiber vibrated by a piezoelectric transducer or through a rotating ground disk. Since the frequency of mechanical motion is low, the temporal coherence of the light is not affected. Although these methods for speckle reduction have been reported in literature, there are no commercially available instruments that implement them. For this reason, we developed a custom device. We chose the rotating disk approach due to its simplicity.

Figure 2(a) shows the assembled light source. The laser is a 130 mW single-mode laser diode with a wavelength of 660 nm (Mitsubishi Electric, Cypress, CA). It is mounted on a heat sink and cooled by a fan. The laser output is collimated by a lens and passed through a diffusive plastic disk mounted on a 2000 rpm electric motor. The light is then collected by a fiber bundle and guided to an illumination port of the Veeco NT1100 [Fig. 2(b)]. Approximately 90% of the laser light is lost in this setup due to the scattering by the rotating disk. However, the coupled light is still sufficient for imaging at any magnification, and the laser diode is run well below its peak power.

The frequency of random modulation of the light by the disk depends on the roughness profile of the disk and the rotation speed. We estimate that this frequency is less than 1 MHz, which would limit coherence time to 1 μs and coherence length to 300 m. Since our application requires coherence length only on the order of millimeters (Table I), any limitation in temporal coherence by the spinning disk is insignificant. At the same time, the random modulation frequency is much higher than the sampling frequency of the Veeco NT1100 CCD (30 Hz). Therefore, the speckle pattern appears averaged out to the CCD. Figure 3 shows images of a sample illuminated by the laser with the disk rotation off or on. In the first case, the speckle degrades the image severely; in the second case, the speckle is eliminated, allowing the sample features and interference fringes to be clearly resolved.

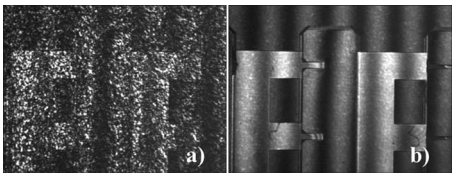

FIG. 3. Interference intensity image of a sample (cantilevers over a trench) taken by the Veeco NT1100 with laser illumination. (a) The light is temporally and spatially coherent. (b) The light is decohered spatially by passing it through the rotating disk.

IV. MEASUREMENT RESULTS

The modified Veeco NT1100 profiler was tested with samples covered by glass or water. First, we present intensity images to show that interference contrast is still high despite the refractive media. Next, height measurements in PSI mode are presented and compared to results obtained without any material covering the sample. In all experiments, the sample is a gold-coated silicon nitride cantilever with nominal dimensions of 100×30 μm^2. The cantilever is bent upward due to residual stress gradient in the material; the tip is about 1.5 μm above the base. The measurements in liquid are performed by immersing the chip in a Petri dish with de-ionized water. The liquid level is adjusted to be approximately 3 mm above the sample surface using a pipette. For measurements under glass, the chip is covered with a 500 μm thick Pyrex slab positioned 1 mm above the sample surface using spacers. The profiler is set to a compound magnification of $40\times$ in all experiments described.

A. Interference contrast

Contrast is used as a figure of merit of the interference pattern since it impacts directly the accuracy of a PSI measurement described by Eq. (1). Contrast is given as $(I_{max}-I_{min})/(I_{max}+I_{min})$, where I_{max} and I_{min} are the intensities of the interference maxima and minima, respectively.

Figure 4 shows a set of grayscale intensity images and the calculated interference contrast for a sample under different conditions. In images (a)–(c), the original built-in illumination source of the Veeco NT1100 is used. This yields considerable contrast when the sample is in air (a) but no measurable contrast when the sample is covered by water or glass [(b) and (c)]. Therefore, interferometric measurement is not possible in the latter cases. In images (d) and (e), the laser with a rotating diffuser is used for illumination. This boosts the interference contrast in air (d) compared to the original source, and, more importantly, enables measurable interference contrast for samples under water or glass [(e) and (f)]. Although the contrast through the refractive media is reduced, it still allows accurate interferometric measurements, as will be shown in Sec. IV B.

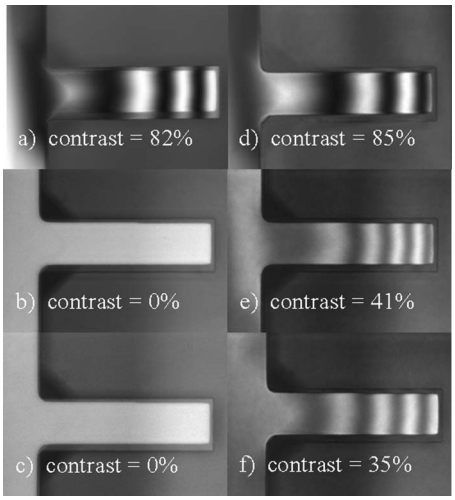

FIG. 4. Interference images of sample under different conditions: (a) original profiler, uncovered sample, (b) original profiler, sample under 3 mm water, (c) original profiler, sample under 500 μm of glass, (d) upgraded profiler, sample uncovered, (e) upgraded profiler, sample under 3 mm water, and (f) upgraded profiler, sample under 500 μm glass.

B. Height measurements

PSI measurements were performed through glass and water to estimate the impact of the reduced interference contrast. Note that the profiler software assumes that the original light source is being used and the wavelength is approximately 606 nm. Therefore, the results given by the software must be multiplied by a calibration factor to take into account the different wavelengths of the laser diode (660 nm) and the different refractive indices of the medium. For measurements through glass, the height changes in the sample occur in air, and no refractive index adjustment is necessary [Fig. 5(a)]. The theoretical calibration factor in that case is 1.09. For measurements through water, the height changes in the sample occur in water with a refractive index of 1.33 [Fig. 5(b)]; the theoretical calibration factor becomes 0.82. The calibration factors were empirically determined to be 1.06 for air and 0.80 for water. The slight discrepancy between the theoretical and actual factors may be due to the differences between the datasheet values and the actual wavelengths of the light sources in use. The empirical factors were used for scaling all measurements reported here.

Figure 6 shows a line scan of the sample through air and through refractive materials (multiplied by the calibration factor). This is essentially a height map along a line in the middle of the cantilever, spanning the cantilever length. The measurement through water and glass agrees closely with those of the uncovered sample over the whole height range. This demonstrates that, as expected, the same calibration factor can be used for all heights, and that the measurement accuracy is not significantly affected by the refractive media.

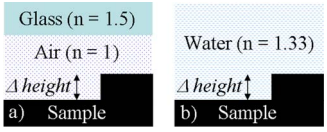

FIG. 5. (Color online) (a) For measurements through glass, the sample surface is covered by air and height changes occur in air. (b) For measurements through water, the sample surface is covered by water and height changes occur in water.

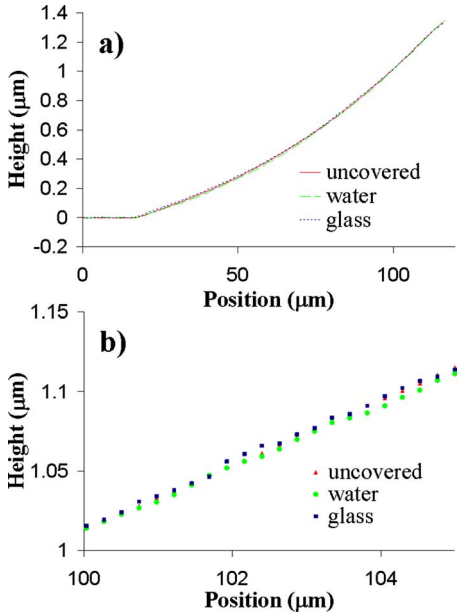

FIG. 6. (Color online) (a) Line scans of uncovered sample using original profiler and of water-covered or glass-covered samples using upgraded profiler. The water and glass thickness are 3 mm and 500 μm, respectively. (b) Magnified section of plot in (a).

To allow a more quantitative analysis, Table II shows the results of multiple height measurements of the sample at three different points. Points A–C are located 30, 65, and 100 μm from the base of the cantilever, respectively. The width of the cantilever is also measured. Again, the measurements are performed with the original profiler on an uncovered sample and with the upgraded profiler through 3 mm of water or 500 μm of glass. Several important observations can be made from these results.

The measurement precision is degraded by the glass more than by the water (note the increase in the standard deviation in each case in Table II). This trend is consistent

TABLE II. Point height measurements and width measurement of uncovered and covered samples. Each value is the average of 30 measurements, and a standard deviation is given. The discrepancy is the difference between the average values of the covered sample and that of the uncovered sample. Heights are in nanometers and widths are in micrometers.

	Uncovered	Water	Glass
Calibration factor used		0.80	1.06
Height of point A	106.2	111.0	104.5
Standard deviation	4.3	5.8	9.4
Discrepancy	···	4.8	−1.7
Height of point B	477.3	480.7	465.9
Standard deviation	8.0	11.9	18.3
Discrepancy	···	3.4	−11.4
Height of point C	1024.2	1033.1	1007.3
Standard deviation	11.3	16.1	26.0
Discrepancy	···	8.9	−16.9
Width of cantilever (μm)	28.1	28.4	27.9
Standard deviation	0.03	0.08	0.17
Discrepancy	···	0.3	−0.2

with the results in Fig. 4, where the interference contrast is reduced more by glass than by water. Although the glass is thinner than the water, it has a higher refractive index (1.5 compared to 1.33). This causes more reflections at the interface, reducing the interference contrast, and more image distortion, reducing the optical resolution. The measurement precision is also degraded by increasing the sample height. Point C has a higher standard deviation than B and A in all cases. However, this trend is normal for PSI measurements; note that it occurs for the uncovered sample as well.

Unlike the precision, the measurement accuracy does not follow a clear pattern. We assume that the measured value using the uncovered sample is correct. Then, the discrepancy between the uncovered and covered samples gives the accuracy of the measurement through the refractive media. Table II shows that the discrepancies for glass are higher than those for water only in some cases. Also, the increase in sample height leads to increased discrepancy in some cases but not in others. The lack of a clear trend in accuracy suggests that part of the error may be due to imperfect sample positioning. Slightly different points on the sample with different heights are measured when transitioning from the uncovered to water-covered to glass-covered setups. This adds to the overall discrepancy and masks any underlying trends in instrument accuracy through the refractive media. Note that the positioning error is not caused by the refractive media; it also occurs for uncovered samples if they are moved between measurements.

V. DISCUSSION

The estimated coherence length of the laser source is very large (Table I), and the interference contrast through water and glass should not be noticeably affected by the increased OPD. However, the experimental results clearly show a drop in contrast and an associated reduction in measurement precision. We attribute this decrease to the intensity mismatch between the sample and reference beams forming the interference image. The refractive material causes a reflection at the material/air interface, reducing the sample beam intensity. Using Eq. (1), it can be shown that interference contrast is maximized when $I_1=I_2$. Therefore, the contrast through refractive media can be improved by manufacturing interferometric objectives with adjustable beam splitter ratio or reference mirror reflectivity.

Although the results show a clear reduction in measurement precision, this reduction is small. The standard deviation is increased by approximately a factor of 2 in the case of glass and 1.5 in the case of water. The discrepancy between height measurements of uncovered and covered samples is less that 17 nm (that may be caused by sample positioning errors and not instrument errors alone). This performance is quite satisfactory for typical MEMS applications. For example, we have used the upgraded Veeco NT1100 profiler to measure the response of a cantilever biosensor in liquid.[26,27] The cantilever was coated with a responsive polymer, causing it to bend when exposed to certain biomolecules in a sample solution. The laser illumination source allowed us to characterize the sensor performance in solution, which was not possible with the original configuration of the profiler.

PSI has a limited vertical range. For this reason, optical profilers also have a VSI capability with lower precision but much higher range. This approach relies on light with short coherence length to make the interference contrast highly dependent on OPD. Therefore, our method of measuring through refractive media by increasing the coherence length is not applicable to VSI.

For PSI measurements, the largest allowable height difference between adjacent pixels in the image is a quarter-wavelength. The interference intensity is a periodic function of OPD as shown in Eq. (1); path differences larger than one period cannot be uniquely determined due to the multiple solutions of the equation. As a result, the maximum step height measurable by PSI is approximately 150 nm. However, if the sample has a sloping profile rather than an abrupt step, the total height difference is distributed over multiple pixels. This allows heights much larger than 150 nm to be measured provided that the sample surface remains in the depth of focus of the objective. We have been able to measure heights exceeding 15 μm for such samples (the maximum height depends on the slope and magnification). As discussed in Sec. I, profiler measurements through packaging or liquid typically need to be performed only on movable MEMS structures, such as cantilevers, bridges, and membranes. These structures have a sloping profile and, therefore, can be readily imaged by PSI.

In this work, we limited the thickness of the refractive materials covering the sample to 3 mm for water and 500 μm for glass. These thicknesses are sufficient for immersing a MEMS device in liquid or packaging it hermetically. Our upgraded profiler can also measure through thicker materials, but the error becomes increasingly larger due to blurring of the image. Note that this problem is not specific to profilers and impacts optical microscopes in general. Using objectives with lower numerical apertures can reduce the adverse effect of the transparent material at the expense of the magnification. For profiling through very thick refractive media, however, a corrected objective would be necessary, similar to the coverslip-corrected objectives used in conventional optical microscopy.

VI. CONCLUSIONS

This paper presents the modification of an optical profiler based on PSI to enable measurements through transparent media. Its original illumination source was replaced by a laser to reduce the linewidth and increase the temporal coherence of the light. The laser beam was spatially decohered with a custom-made rotating diffuser to reduce speckle noise. The upgraded instrument was tested by profiling samples covered with water or glass, and these results were compared to measurements of uncovered samples with the unmodified instrument. The measurement precision is degraded by the transparent materials but not significantly. The upgraded profiler has been successfully used to characterize the response of a cantilever biosensor in liquid,[26,27] and many other MEMS applications could benefit from this

method. We hope that optical profiler manufacturers will take this work into consideration when designing the next generation of their instruments.

ACKNOWLEDGMENTS

This work was funded by the Laboratory for Physical Sciences (LPS) and the R. W. Deutsch Foundation. The authors would also like to thank colleagues at the MEMS Sensors and Actuators Laboratory (MSAL) at the University of Maryland for useful discussions.

[1] A. Bosseboeuf and S. Petitgrand, Proc. SPIE **5145**, 1 (2003).
[2] D. Grigg, E. Felkel, J. Roth, X. C. d. Lega, L. Deck, and P. J. de Groot, Proc. SPIE **5455**, 429 (2004).
[3] X. Hu, G. Liu, C. Hu, T. Guo, and X. Hu, Meas. Sci. Technol. **17**, 1312 (2006).
[4] S. Jorez, A. Cornet, and J.-P. Raskin, Opt. Commun. **263**, 6 (2006).
[5] G. Udupa, M. Singaperumal, R. S. Sirohi, and M. P. Kothiyal, Meas. Sci. Technol. **11**, 315 (2000).
[6] R. Artigas, A. Pinto, and F. Laguarta, Proc. SPIE **3824**, 93 (1999).
[7] Y. L. Low, R. E. Scotti, D. A. Ramsey, C. A. Bolle, S. P. O'Neill, and K. C. Nguyen, J. Electron. Packag. **125**, 325 (2003).
[8] D. Sparks, J. Trevino, S. Massoud-Ansari, and N. Najafi, J. Micromech. Microeng. **16**, 2488 (2006).
[9] J. W. L. Zhou, H.-Y. Chan, T. K. H. To, K. W. C. Lai, and W. J. Li, IEEE/ASME Trans. Mechatron. **9**, 334 (2004).
[10] N. Chronis and L. P. Lee, J. Microelectromech. Syst. **14**, 857 (2005).
[11] R. McKendry, J. Zhang, Y. Arntz, T. Strunz, M. Hegner, H. P. Lang, M. K. Baller, U. Certa, E. Meyer, H.-J. Guntherodt, and C. Gerber, Proc. Natl. Acad. Sci. U.S.A. **99**, 9783 (2002).
[12] N. V. Lavrik, M. J. Sepniak, and P. G. Datskos, Rev. Sci. Instrum. **75**, 2229 (2004).
[13] S. Han and T. Browne, Proceedings of the International Symposium on Advanced Packaging Materials: Processes, Properties and Interfaces, 2005 (unpublished), p. 13.
[14] S. Han, Proc. SPIE **6032**, 603203 (2006).
[15] S. Han, Proc. SPIE **6149**, 614901 (2006).
[16] B. Dingel and S. Kawata, Opt. Lett. **18**, 549 (1993).
[17] D. Malacara, *Optical Shop Testing*, 3rd ed. (Wiley, Hoboken, NJ, 2007).
[18] P. de Groot, Appl. Opt. **39**, 2658 (2000).
[19] J. F. Biegen, U.S. Patent No. 4,732,483 (22 March 1988).
[20] Y. Ishii, J. Chen, R. Onodera, and T. Nakamura, Opt. Eng. **42**, 60 (2003).
[21] A. Harasaki, J. Schmit, and J. C. Wyant, Appl. Opt. **39**, 2107 (2000).
[22] P. Goldberg, P. W. Milonni, and B. Sundaram, Phys. Rev. A **44**, 1969 (1991).
[23] M. Mansuripur, *Classical Optics and its Applications* (Cambridge University Press, Cambridge, England, 2002).
[24] T. Iwai and T. Asakura, Proc. IEEE **84**, 765 (1996).
[25] L. Wang, T. Tschudi, T. Halldorsson, and P. Petursson, Opt. Eng. **39**, 1659 (2000).
[26] S. T. Koev, M. A. Powers, H. Yi, L.-Q. Wu, W. E. Bentley, G. W. Rubloff, G. F. Payne, and R. Ghodssi, Lab Chip **7**, 103 (2007).
[27] S. T. Koev, L.-Q. Wu, G. F. Payne, and R. Ghodssi, Proceedings of the Tenth International Conference on Miniaturized Chemical and Biochemical Analysis Systems, 2006 (unpublished), p. 1250.